



Cite this: *J. Mater. Chem. B*, 2020, **8**, 282

Amphiphilic phthalocyanines in polymeric micelles: a supramolecular approach toward efficient third-generation photosensitizers†

Francesca Setaro,^a Jos W. H. Wennink,^b Petri I. Mäkinen,^c Lari Holappa,^c Panagiotis N. Trohopoulos,^d Seppo Ylä-Herttua,^c Cornelius F. van Nostrum,^{*b} Andres de la Escosura ^{*ae} and Tomas Torres ^{*aef}Received 16th September 2019,
Accepted 25th November 2019

DOI: 10.1039/c9tb02014d

rsc.li/materials-b

In this paper we describe a straightforward supramolecular strategy to encapsulate silicon phthalocyanine (SiPc) photosensitizers (PS) in polymeric micelles made of poly(ϵ -caprolactone)-*b*-methoxypoly(ethylene glycol) (PCL-PEG) block copolymers. While PCL-PEG micelles are promising nanocarriers based on their biocompatibility and biodegradability, the design of our new PS favors their encapsulation. In particular, they combine two axial benzoyl substituents, each of them carrying either three hydrophilic methoxy-(triethylenoxy) chains (**1**), three hydrophobic dodecyloxy chains (**3**), or both kinds of chains (**2**). The SiPc derivatives **1** and **2** are therefore amphiphilic, with the SiPc unit contributing to the hydrophobic core, while lipophilicity increases along the series, making it possible to correlate the loading efficacy in PCL-PEG micelles with the hydrophobic/hydrophilic balance of the PS structure. This has led to a new kind of third-generation nano-PS that efficiently photogenerates $^1\text{O}_2$, while preliminary *in vitro* experiments demonstrate an excellent cellular uptake and a promising PDT activity.

1. Introduction

The use of nanotechnology for medical purposes has grown exponentially over the past few decades. Research efforts in nanomedicine aim at developing nanostructured systems for therapy, diagnosis and therapy monitoring applications.¹ In the field of photodynamic therapy (PDT), for example, third-generation photosensitizers (PS) are composed of a second-generation PS conjugated to or encapsulated in biodegradable/biocompatible nanoparticles, which broadens the PS clinical potential.^{2–4} Third-generation PS circumvent some of the deficiencies relative to second-generation PS, improving their pharmacokinetics,

pharmacodynamics and biodistribution *in vivo*. In this respect, various nanoparticle types have been used as PS carriers, including the very promising polymeric micelles.^{5–7} Advances in fiber-optic based laser technologies also make feasible a highly selective local PS activation, even in deep and scarcely accessible tissues.

Phthalocyanines (Pc)^{8–12} constitute one of the most promising families of second-generation PS. An important advantage of Pc, in comparison to other porphyrinoid PS, is their intense absorption within the therapeutic window.^{13–18} The absorption Q-band of Pc is almost two orders of magnitude more intense than the highest Q-band of haematoporphyrin, while they show hardly any absorption in the range of 400–600 nm. Furthermore, Pc present high quantum yields and long lifetimes of their triplet excited state, which assist in the generation of singlet oxygen ($^1\text{O}_2$). A shortcoming of Pc in this field is, however, the strong tendency of their aromatic ring to aggregate, especially in water and aqueous buffered solutions, leading to a decrease or total loss of their photosensitizing capability.¹⁹ Consequently, one of the main challenges for chemists working on this topic is to synthesize Pc with a low aggregation tendency¹⁷ or, likewise, to embed them in nanosized architectures able to disrupt the aggregates.^{20–22} Besides, Pc are hydrophobic compounds, which decreases their solubility in aqueous media. This problem can be solved by pure chemical means, *i.e.*, through the inclusion of hydrophilic groups,¹⁹ or by encapsulation into water-dispersible nanocarriers.^{2–4} Polyester-based nanocarriers are the most suitable

^a Organic Chemistry Department, Universidad Autónoma de Madrid, 28049 Cantoblanco, Madrid, Spain. E-mail: andres.delaescosura@uam.es, tomas.torres@uam.es

^b Department of Pharmaceutics, Utrecht Institute for Pharmaceutical Sciences (UIPS), Utrecht University, Universiteitsweg 99, 3508 TB Utrecht, The Netherlands. E-mail: C.F.vanNostrum@uu.nl

^c A.I. Virtanen Institute for Molecular Sciences, University of Eastern Finland, Neulaniementie 2, Kuopio FIN-70211, Finland

^d CosmoPHOS Ltd, 77 Tsimiski str., GR – 54622, Thessaloniki, Greece

^e Institute for Advanced Research in Chemical Sciences (IAdChem),

28049 Cantoblanco, Madrid, Spain

^f IMDEA Nanoscience, Ciudad Universitaria de Cantoblanco, 28049 Madrid, Spain

† Electronic supplementary information (ESI) available: Synthesis and characterization of PS compounds and block copolymers; singlet oxygen studies; and study of PS-loaded polymeric micelles. See DOI: 10.1039/c9tb02014d

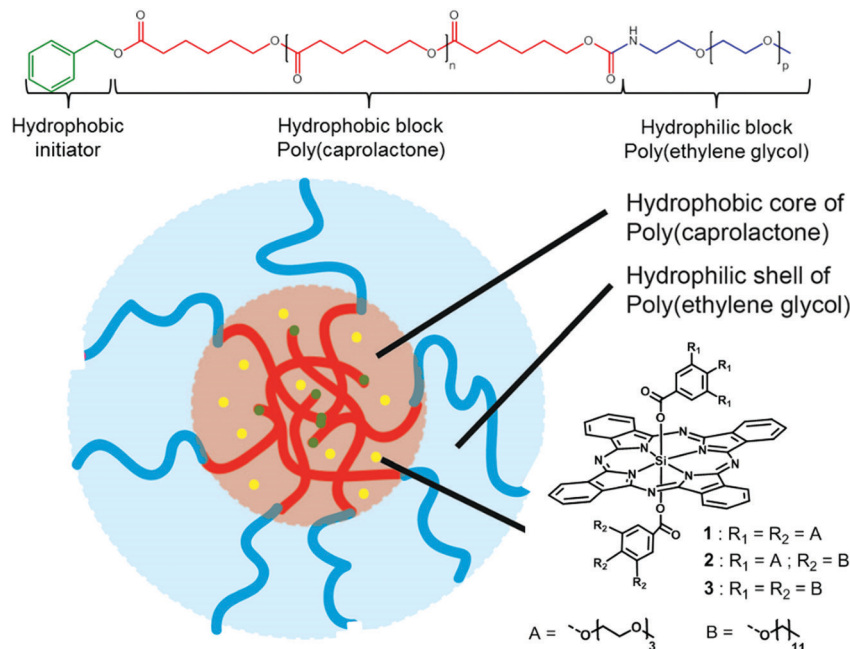


Fig. 1 Schematic representation of the proposed strategy toward third-generation PS based on the encapsulation of amphiphilic SiPc derivatives (compounds **1** and **2**, while **3** serves as a reference lipophilic derivative) in PCL-PEG polymeric micelles.

ones for that purpose considering their biocompatibility and biodegradability. Among them, micelle forming block copolymers of polyethylene glycol and polylactic acid (PLA-PEG)²³ or poly(ϵ -caprolactone) (PCL-PEG)²⁴ are the most frequently investigated.

For instance, PCL-PEG micelles have been successfully implemented for the efficient solubilization and enzymatically controlled release of temoporfin (mTHPC),^{25,26} a PS clinically used in PDT of head and neck cancers. Importantly, the introduction of aromatic groups in the polymer chain can strongly aid in the encapsulation of the PS through aromatic π - π stacking interactions,²⁷ for example by substitution of the PCL chain ends by aromatic groups (benzyl or naphthyl).²⁵

On these bases, herein we describe the incorporation of novel amphiphilic silicon Pc (SiPc) compounds into polymeric micelles formed by block copolymers of benzyl or naphthyl substituted poly(ϵ -caprolactone)-*b*-methoxypoly(ethylene glycol) (ben-PCL-PEG and nap-PCL-PEG, respectively) and their use as efficient third-generation PS (Fig. 1). The supramolecular character of this encapsulation strategy renders it simple from the synthetic point of view, and gentle regarding the conditions required for micelle loading. In the PCL-PEG micelles, the hydrophobic polyester segments are located in the micellar core, allowing the PS to locate at such core or across the core-shell interface, depending on the PS nature. We will show in this paper that tuning the hydrophilic/hydrophobic balance of the SiPc axial substituents, or the (aromatic) chain end and polyester block lengths in the micellar structure, allows optimizing both the loading efficiency and PS aggregation inside the micelles, thus enhancing the observed photodynamic effect. To prove the utility of such an approach, we also show proof of concept of the excellent *in vitro* PDT efficacy and cellular uptake of these promising third-generation PS.

2. Experimental section

The list of instruments, materials, synthetic methods for the preparation of SiPc **1**–**3** and micellar block copolymers, characterization of the compounds, and singlet oxygen generation capacity of the three PS, are listed in the ESI.†

2.1. Protocol for micelle formation

Pure micelles and those loaded with SiPc compounds **1**–**3** were formed by the film hydration method.²⁵ In short, 10 mg of ben-PCL-mPEG or nap-PCL-mPEG block copolymers were dissolved in 1 mL of dichloromethane. 5 mg of SiPc compound **1**, **2** or **3** were dissolved in 1 mL of THF and different amounts corresponding to the desired polymer/PS ratios were mixed with the dichloromethane block copolymer solution. By evaporation of dichloromethane and THF a thin solid film was formed. The formed film contained both block copolymers and homogeneously distributed PS. The block copolymer (plus PS) film was subsequently dissolved in 1 mL PBS solution by gentle shaking and after 1 hour filtered through a 0.2 μm syringe filter, to remove non-encapsulated and thus precipitated SiPc. This procedure results in empty micelles or PS loaded micellar solutions of 10 mg mL⁻¹ ben-PCL_{*n*}-mPEG₄₅ or nap-PCL_{*n*}-mPEG₄₅.

2.2. Procedure to determine loading efficiency and loading capacity

The concentration of SiPc compounds **13** in micellar dispersions was determined by UV-Vis spectroscopy. The dispersions were diluted in DMF to dissolve the micelles. A spectrum between 300 nm and 800 nm was recorded by a Shimadzu UV-2450 spectrophotometer (Shimadzu, Japan). The absorbance at 686 nm was analyzed against a calibration curve of SiPc **1**–**3** in DMF, which was

linear between 0 and $6 \mu\text{g mL}^{-1}$. The loading efficiency (LE) and loading capacity (LC) were calculated by eqn (1) and (2), respectively.

$$\text{LE (\%)} = \frac{\text{SiPc compounds 1–3 loaded (mg)}}{\text{SiPc compounds 1–3 fed (mg)}} \times 100\% \quad (1)$$

LC (%)

$$= \frac{\text{SiPc compounds 1–3 loaded (mg)}}{\text{polymer used (mg) + SiPc compounds 1–3 loaded (mg)}} \times 100\% \quad (2)$$

2.3. *In vitro* biological studies

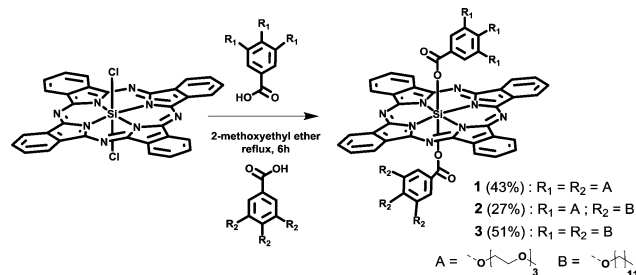
For photodynamic cell-killing experiments, mouse macrophage RAW264.7 (ATCC; TIB-71) cell line was cultured in Dulbecco's Modified Eagle's Medium (DMEM) supplemented with 10% FBS, 1% penicillin–streptomycin. The cell killing efficacy of the different micellar compositions was analyzed using MTS-assay (Promega). Cells were first split into a 96-well plate, and one day later the PS-micellar hybrids were applied to the cells and subsequently allowed to incubate with the cells for 2 h. After this, cells were illuminated with a custom-made LED device emitting light at 670 nm wavelength for 10 minutes, with LED light intensity of 3.04 mW cm^{-2} . 24 hours later MTS-reagent was applied to the plate, and measured one hour later by spectrophotometry (Multiskan Ascent, MTX LabSystems). Cells without PS-micellar compositions and without light activation were always used as a control.

For fluorescence microscopy, cells were split into chamber slides. One day later, the PS-micelle hybrids were applied to the cells. After 2 h of incubation, cells were rinsed with PBS and fixed with 1% paraformaldehyde. Images were taken with Nikon Eclipse Ni-e (Nikon Corporation, Japan).

3. Results and discussion

3.1. Synthesis and characterization of amphiphilic SiPc-based PS

As PS, we have chosen to use SiPc derivatives because they have a proven clinical potential for PDT, and their properties can be tuned through the introduction of different substituents at axial positions of the Pc macrocycle.^{28–33} The target SiPc compounds (1–3, see Fig. 1) bear two axial benzoyl substituents, each of them with either three methoxy(triethylenoxy) chains (1), three dodecyloxy chains (3), or both kinds of chains (2). Consequently, the SiPc derivatives 1 and 2 are amphiphilic, with the SiPc unit contributing to the hydrophobic core, while lipophilicity increases along the series, making possible to correlate the loading efficacy in PCL–PEG micelles with the hydrophobic/hydrophilic balance of the PS structure. The synthesis of 1–3 (for details: see ESI†) took place by nucleophilic displacement of the chlorine atoms from the commercially available silicon phthalocyanine dichloride (SiPcCl_2) with an excess of the corresponding benzoic acid derivatives (up to 10 eq., in a 1:1 mixture for the case of 3) under reflux of 2-methoxyethyl ether for 6 h (Scheme 1). The compounds were



Scheme 1 Synthesis of the SiPc derivatives 1–3.

then purified by column chromatography, using mixtures of DCM and methanol as eluent, and fully characterized by NMR (Fig. S1, ESI†), UV-vis and FT-IR spectroscopies, and MALDI-TOF spectrometry (see ESI†). The solubility of each of these PS is determined by the axial substituents. SiPc 1 is for example soluble in polar solvents, including water, while in non-polar solvents it forms a gummy solid that is impossible to filter. SiPc 2, in turn, is soluble in a range of polar and non-polar solvents such as methanol, acetone, THF, DCM and hexane. Finally, the lipophilic SiPc 3 is only soluble in non-polar organic solvents such as DCM and hexane, and serves in our study as a reference compound.

The UV/vis spectra of compounds 1, 2 and 3 were initially recorded in chloroform (Fig. 2a), where, despite its non-coordinating nature, they are clearly non-aggregated, as revealed by the sharp

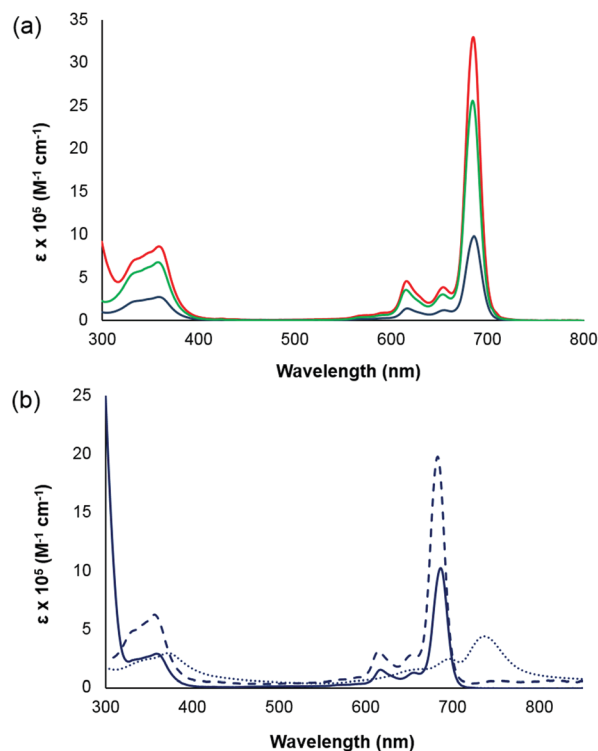


Fig. 2 (a) UV-vis spectra of compounds 1 (blue), 2 (green) and 3 (red) in chloroform ($M = 2 \times 10^{-6} \text{ mol L}^{-1}$). (b) UV-vis spectra of the SiPc 1 in chloroform (solid line, $M = 2 \times 10^{-6} \text{ mol L}^{-1}$), methanol (dashed line, $M = 2 \times 10^{-6} \text{ mol L}^{-1}$) and water (with 1% methanol) (dotted line, $M = 1 \times 10^{-5} \text{ mol L}^{-1}$).

Q-band present at 686 nm. As expected, increasing the number of methoxy(triethylenoxy) chains decreases the PS absorption intensity, so the extinction coefficient of the amphiphilic species **2** has an intermediate value ($\epsilon = 2.6 \times 10^5 \text{ M}^{-1} \text{ cm}^{-1}$) with respect to the symmetric analogues **3** ($\epsilon = 3.1 \times 10^5 \text{ M}^{-1} \text{ cm}^{-1}$) and **1** ($\epsilon = 1 \times 10^5 \text{ M}^{-1} \text{ cm}^{-1}$). Because compound **1** is hydrophilic, its absorption spectrum could also be recorded in polar solvents (Fig. 2b). In methanol (Fig. 2b, dashed line), the Q-band absorption maximum suffers a slight hypsochromic shift (*i.e.* centered at 683 nm) compared to that obtained in chloroform (*i.e.* centered at 686 nm, solid line). The extinction coefficient value of **1**, in turn, is twice higher in methanol ($\epsilon = 2 \times 10^5 \text{ M}^{-1} \text{ cm}^{-1}$), probably because the compound is better dissolved in this solvent. Importantly, PS **1** is also soluble in aqueous solution, if it is injected from a concentrated solution in MeOH or DMSO (1% of the total volume). As shown in Fig. 2b (dotted line), under these conditions the spectrum changes completely, compared to that in chloroform, with the Q-band presenting two major peaks: one centered at 698 nm, corresponding to the monomeric species, and the main and bathochromically shifted band with maximum absorption at 738 nm, which is probably due to formation of J-aggregates. To explain this result, as for other SiPc derivatives previously reported,^{34–37} we hypothesize that in water **1** assumes a conformation where the hydrophilic part of the molecule is exposed to the polar environment, thus promoting π - π interactions of the aromatic macrocycle and consequently J-type stacking (further discussed below).

In order to assess the photosensitizing ability of our SiPc derivatives in solution, the $^1\text{O}_2$ quantum yields (Φ_Δ) of compounds **1–3** were determined through the relative method,³⁸ based on measuring the rate of photodegradation of a chemical scavenger (1,3-diphenylisobenzofuran – DPBF) that is directly proportional to the formation of $^1\text{O}_2$ (Fig. 3). The measurements were conducted in DMSO, with the exception of SiPc **3**, which for solubility reasons had to be measured in THF. The solvent choice aimed at ensuring that the Pc system remained in a non-aggregated state, a requirement for $^1\text{O}_2$ generation at the maximum PS capacity. Fig. S2 (ESI†) shows as a representative example the decay of the scavenger absorption induced by PS **1** during irradiation, while data for

compounds **2** and **3** were almost identical. Decrease in Q-band intensity or appearance of new bands were not observed in any case, ensuring the PS integrity over the whole experiment.

Under these circumstances, plotting the dependence of $\ln(A_0/A_t)$ against irradiation time (t) (with A_0 and A_t being the respective scavenger absorbance values at the monitoring wavelength before and after the irradiation time t) affords a straight line whose slope reflects the PS efficacy to generate $^1\text{O}_2$, and from which Φ_Δ can be calculated (see ESI†). Taking non-substituted ZnPc as the reference compound ($\Phi_{\Delta(\text{DMSO})} = 0.67$),^{39,40} the scavenger photodegradation profiles induced by the SiPcs **1** and **2** (Fig. 3) correspond to Φ_Δ values of 0.27 and 28, respectively. The Φ_Δ for SiPc **3** was calculated to be 0.27, but it was measured in a different solvent (THF) and so the corresponding plot is not comparable in Fig. 3. The fact that Φ_Δ is almost identical for the three compounds correlates well with the similar chemical features of their axial substituents, only differing by their side chains, which tune the solubility and aggregation properties but do not affect the electronic structure of the SiPc core. For comparison, we also measured the $^1\text{O}_2$ quantum yield of the SiPc derivative Pc **4** in DMSO (Fig. 3, blue data), *i.e.*, the benchmark PS among the family of Pcs.⁴¹ The resulting value ($\Phi_{\Delta(\text{Pc4})} = 0.20$) is lower than those obtained for **1–3**, revealing that the photodynamic behavior of the new SiPcs is at the same level or even superior to the best PS systems in the field of PDT.

3.2. Loading of amphiphilic SiPc-based PS into PCL-PEG micelles

In order to combine the previously synthesized PS with polymeric micelles, a library of Ben-PCL-PEG and Nap-PCL-PEG block copolymers with varying PCL chain lengths (on average 7–19 units) and a fixed PEG block (M_w of 2000 Da) were prepared. These syntheses were carried out through ring opening polymerization of ϵ -caprolactone by benzyl or naphthyl alcohol, respectively, followed by activation of the hydroxyl end group and reaction with amine-terminated ω -methoxypolyethylene glycol (details of synthesis and characterization: see ESI†). The molecular weights of the synthesized mPEG₄₅-NH₂, intermediate PCL polymers and the final Ben-PCL-PEG and Nap-PCL-PEG block copolymers were characterized by GPC, and the results are given in Table S1 and Fig. S3 (ESI†). The GPC chromatograms of Fig. S3A (ESI†) show for example that the Ben-PCL₁₉-OH and mPEG₄₅-NH₂ peaks shift to the new Ben-PCL₁₉-mPEG₄₅ peak and remain narrow. There are no residual peaks visible at the retention times of the mPEG₄₅-NH₂ and Ben-PCL₁₉-OH. These results are indicative for a successful synthesis and coupling reaction.

PS **1–3** loaded micelles of both Ben- and Nap-PCL-PEG were then prepared by the film hydration method.²⁵ First, a solution of the amphiphilic polymer in DCM was mixed with various amounts of a solution of the PS (5 mg mL^{-1}) in THF. The mixture was gently shaken for a minute and the solvents were rotary evaporated, giving rise to a thin film of block copolymer with homogeneously distributed PS. Heating the thin film up to $60 \text{ }^\circ\text{C}$ during subsequent hydration by phosphate buffered saline (PBS, pH 7.4) was necessary to optimize the encapsulation process and to prevent aggregation of the PS. The resulting

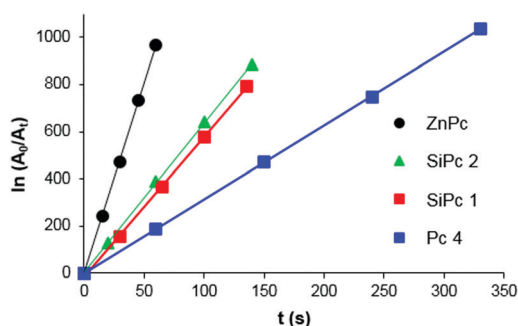


Fig. 3 Plot of the decrease in DPBF absorption with time, photoinduced by non-substituted ZnPc (as reference compound, black data), the SiPc **1** (red data), the SiPc **2** (green data), and the benchmark PS Pc **4** (blue data), which correlates with singlet oxygen produced by each of these PS.

dispersion was filtered through a 200 nm syringe filter to sterilize the solution and remove dust and non-encapsulated PS. Details of this procedure are provided in the Experimental section (see above).

A comprehensive series of hybrid nanosystems were thus prepared, differing in the number of caprolactone repeat units present in the polymer, the aromatic end-group of the poly(caprolactone) chain, the nature of the SiPc compound, and the loading of SiPc in the polymeric micelles (see Table S2, ESI[†]). The amount of encapsulated PS in all prepared compositions was measured by diluting and dissolving the micelles in DMF and measuring PS concentration by UV/vis spectrophotometry, allowing to determine the loading capacity (LC, wt% of SiPc in micelles)

and loading efficiency (LE, % encapsulated with respect to feed %) in each particular case. The results are shown in Fig. S4 and S5 (ESI[†]). TEM and DLS characterization of the micelles was unfortunately impossible, due to their small size and absorption of the DLS wavelength by the PS, respectively. From the data of Fig. S4 and S5 (ESI[†]), it is anyway clear that the most efficient encapsulations were obtained when using Ben-PCL-PEG micelles (compositions 1–20 and 36–44). Among them, the optimum PCL length corresponds to eleven caprolactone monomers, probably because crystallinity of the PCL block increases with chain length, thus hampering encapsulation.²⁶ Concerning the PS, encapsulation of the lipophilic SiPc **3** is highly inefficient (compositions 1–5 and 36–38), while the most hydrophilic SiPc **1** gives rise to the

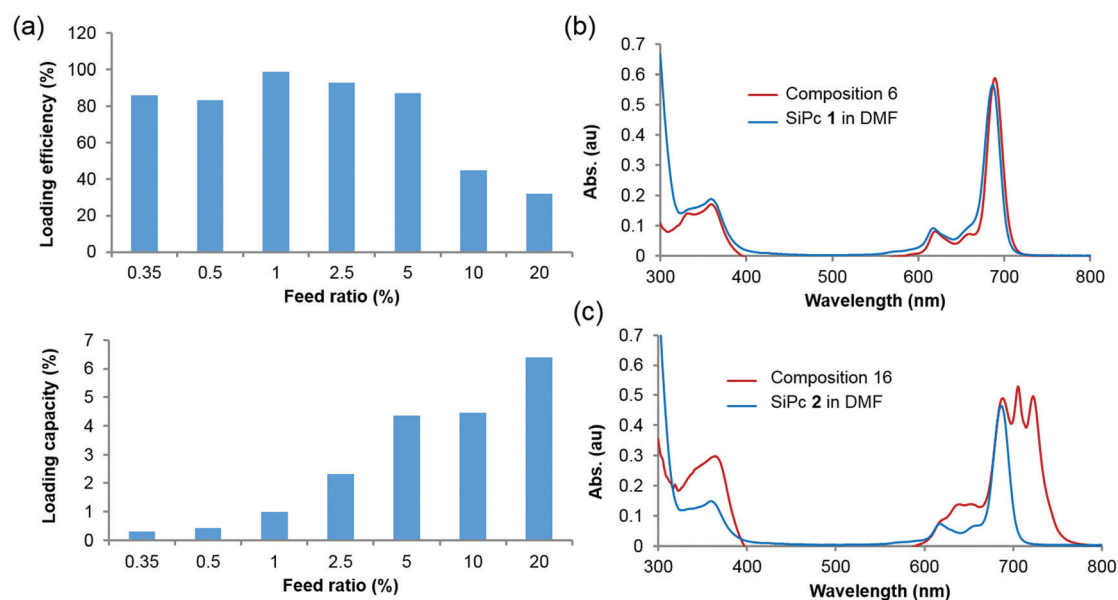


Fig. 4 (a) Loading efficiency (top) and capacity (bottom) of SiPc **1** in PBS-dispersions of Ben-PCL₁₁-PEG polymeric micelles. (b) UV-vis spectra of 6% SiPc **1** in Ben-PCL₁₁-PEG micelles (composition 6, red line) and in DMF (blue line). (c) UV-vis spectra of 1% SiPc **2** in Ben-PCL₁₁-PEG micelles (composition 16, red line) and in DMF (blue line).

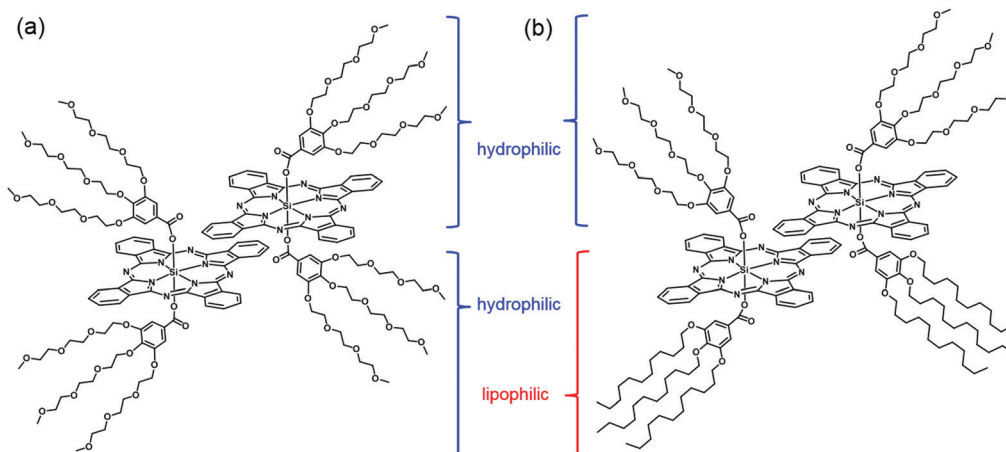


Fig. 5 Proposed hypothetical structure of the supramolecular dimers formed by the amphiphilic SiPc derivatives (a) **1** and (b) **2**. The dimer of **1** has a hydrophilic shell of methoxy(triethylenoxy) chains, in contrast to the amphiphilic character of the monomer, explaining why this compound aggregates in water (see Fig. 2b) but not within the PCL-PEG micelles (Fig. 4b). On the other hand, the dimer of **2** is amphiphilic, thus favoring its formation within micelles, probably at the core-shell interface.

best LC and LE values (compositions 6–15 and 39–41). Loading efficiency was almost quantitative (82–99 wt%) at SiPc **1** to polymer feed ratios of <10 wt%, leading to a proportional increase in loading capacity with increasing feed ratio (Fig. 4a, top). However, loading efficiency decreased when the feed ratio increased to 10 and 20%. Concerning loading capacity, a maximum value of 6% could be obtained (Fig. 4a, bottom).

UV-vis spectroscopy gave information about the aggregation behavior of the SiPc derivatives **1** and **2** within the micellar environment (Fig. 4b and c) compared to that in other solvents where they are soluble (see also Fig. 2). The spectra of compositions containing SiPc **1** in different micellar systems present the characteristic features of non-aggregated SiPc, with a sharp Q-band centered at 686 nm. This effect is illustrated in Fig. 4b, showing the UV-vis spectrum obtained for 6% SiPc **1** in Ben-PCL₁₁-PEG micelles (red line), compared to that of SiPc **1** in DMF (blue line). This is highly advantageous for singlet oxygen production upon illumination and clearly different from the spectrum of SiPc **1** in water as was shown in Fig. 2b. In particular, the spectrum in water shows a red-shift of the Q-band that is indicative of J-aggregate formation,⁴² which supports that in presence of micellar Ben-PCL₁₁-PEG this PS is truly encapsulated in the micelles rather than being dispersed in the aqueous medium. In water, the finding of J-aggregation suggests that the SiPc exists as a hydrophilic supramolecular structure (Fig. 5a), which is not favored upon encapsulation in the PCL-PEG micelles, where the amphiphilic monomer is probably better accommodated at the micellar core-shell interface. On the contrary, micelles of Ben-PCL₁₁-PEG that contain 1% of compound **2** did show a strong PS aggregation, with a clear red shift and splitting of the SiPc Q-band (illustrated in Fig. 4c, red line), as compared to the spectrum of the same PS in DMF (Fig. 4c, blue line) or in chloroform solution (Fig. 2a). Again, these spectral changes are characteristic of Pc J-aggregates. Based on that, Fig. 5b presents a hypothesized scheme of the aggregation mode of this amphiphilic SiPc, likely promoted at the micelles core-shell interface.

3.3. *In vitro* studies

Once the best couple of PS and micellar carrier was chosen (SiPc **1**/Ben-PCL₁₁-PEG), we proceeded to study the PDT potential of the resulting third-generation PS at the highest feed ratio (20%, with 6% LC). The ability of this nano-PS to induce cell killing was studied in a mouse macrophage cell line RAW 264.7, as macrophages play a prominent role in atherosclerosis,⁴³ and in malignancy in the stromal and leukocyte compartment. Distinct macrophage subsets have also been described in cancer,⁴⁴ for which RAW 264.7 cells constitute a good model system for the *in vitro* study of both atherosclerosis and cancer PDT. For the experiment, a custom-made LED device ($\lambda = 670$ nm) for illuminating individual cells on a 96-well plate was used. The illumination time was 10 minutes, with a LED light intensity of 3.04 mW cm⁻². Cells without nano-PS and/or without light activation were used as a control. Besides, a wide range of dilution series was tested, and cells were incubated 24 hours after LED-illumination before measuring the photocytotoxicity. The IC₅₀-value determined from these experiments was approx. 35 ng μL^{-1} of polymeric

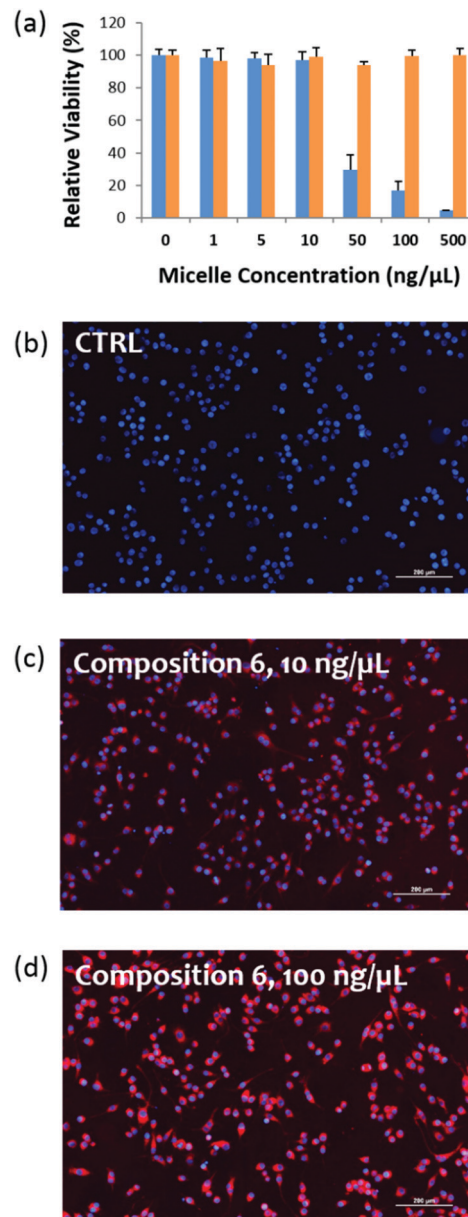


Fig. 6 (a) Cell killing induced by 6% SiPc **1**/Ben-PCL₁₁-PEG micelles (composition 6) in RAW-cells. The viability of the cells was measured by MTS-assay (Promega) after 10 min LED illumination (3.04 mW cm⁻², blue bars) or without illumination (dark toxicity, orange bars). (b–d) Fluorescent microscopy images from RAW cells after treatment with 6% SiPc **1**/Ben-PCL₁₁-PEG micelles at (c) 10 ng μL^{-1} and (d) 100 ng μL^{-1} . Cells without nano-PS serve as controls (CTRL, panel b). Scale bar 200 μm .

micelles (corresponding to 1.2 μM of SiPc **1**), while no dark toxicity was observed up to concentration of 500 ng μL^{-1} (Fig. 6a).

Finally, cellular uptake studies were performed for the SiPc **1**/ben-PCL₁₁-PEG hybrid nano-PS. The ability of SiPc **1** to enter the macrophage cells was analyzed by fluorescence microscopy. Fig. 6b–d shows fluorescent microscopy images from RAW cells after 2 h incubation with 6% SiPc **1**/Ben-PCL₁₁-PEG micelles. Cells without nano-PS serve as controls (CTRL, Fig. 6b). As seen from Fig. 6c, the red fluorescence indicates that at a concentration of 10 ng μL^{-1} a majority of cells contain the fluorescent nano-PS.

Furthermore, 100 ng μL^{-1} concentration leads to strong fluorescence seen in all cells (Fig. 6d). This result, together with the above phototoxicity data, demonstrate the promising PDT potential of the studied nano-PS, as compared to other standards in the field.

4. Conclusions

In summary, herein we have developed a series of SiPc silyl ester derivatives with increasing hydrophilicity of their axial substituents, which in the case of compounds **1** and **2** resulted in amphiphilic PS that can efficiently be incorporated into polymeric micelles by supramolecular means. The best loading efficiency and loading capacity values have been observed for the SiPc **1**, with the additional advantage that it does not aggregate within the micellar environment, thus preserving its photosensitizing properties intact. Consequently, the resulting nanosystem is an efficient third-generation PS, as demonstrated by *in vitro* PDT and cellular uptake experiments using a model macrophage cell line. *In vivo* experiments will be devoted in the future to clarify its clinical potential.

Conflicts of interest

There are no conflicts to declare.

Acknowledgements

This work was supported by EU (CosmoPHOS-nano, EU-FP7-NMP-2012-LARGE-6, 310337), the Spanish MINECO (CTQ2017-85393-P (TT), CTQ-2014-53673-P and CTQ-2017-89539-P (AdIE), PCIN-2017-042/EuroNanoMed2017-191, TEMPEAT (TT)), and Finnish Cultural Foundation. IMDEA Nanociencia acknowledges support from the 'Severo Ochoa' Programme for Centres of Excellence in R&D (MINECO, Grant SEV-2016-0686).

References

- 1 T. L. Doane and C. Burda, The unique role of nanoparticles in nanomedicine: imaging, drug delivery and therapy, *Chem. Soc. Rev.*, 2012, **41**, 2885–2911.
- 2 V. Almeida-Marrero, E. van de Winckle, E. Anaya-Plaza, T. Torres and A. de la Escosura, Porphyrinoid biohybrid materials as an emerging toolbox for biomedical light management, *Chem. Soc. Rev.*, 2018, **47**, 7369–7400.
- 3 J. F. Lovell, T. W. B. Liu, J. Chen and G. Zheng, Activatable photosensitizers for imaging and therapy, *Chem. Rev.*, 2010, **110**, 2839–2857.
- 4 F. Dumoulin, *Photosensitizers in Medicine, Environment and Security*, Springer, New York, 2012.
- 5 C. F. Van Nostrum, Polymeric micelles to deliver photosensitizers for photodynamic therapy, *Adv. Drug Delivery Rev.*, 2004, **56**, 9–16.
- 6 P. Avci, S. S. Erdem and M. R. Hamblin, Photodynamic therapy: one step ahead with self-assembled nanoparticles, *J. Biomed. Nanotechnol.*, 2014, **10**, 1937–1952.
- 7 S. G. Kandekar, S. del Rio-Sancho, M. Lapteva and Y. N. Kalia, Selective delivery of adapalene to the human hair follicle under finite dose conditions using polymeric micelle nanocarriers, *Nanoscale*, 2018, **10**, 1099–1110.
- 8 J. A. A. W. Elemans, R. Van Hameren, R. J. M. Nolte and A. E. Rowan, Molecular materials by self-assembly of porphyrins, phthalocyanines and perylenes, *Adv. Mater.*, 2006, **18**, 1251–1266.
- 9 H. Lu and N. Kobayashi, Optically active porphyrin and phthalocyanine systems, *Chem. Rev.*, 2016, **106**, 6184–6261.
- 10 M. V. Martínez-Díaz, G. de la Torre and T. Torres, Lighting porphyrins and phthalocyanines for molecular photovoltaics, *Chem. Commun.*, 2010, **46**, 7090–7108.
- 11 T. Basova, A. Hassan, M. Durmus, A. G. Gürek and V. Ahsen, Liquid crystalline metal phthalocyanines: structural organization on the substrate surface, *Coord. Chem. Rev.*, 2016, **310**, 131–153.
- 12 M. Bayda, F. Dumoulin, G. L. Hug, J. Koput, R. Gorniaka and A. Wojcik, Fluorescent H-aggregates of an asymmetrically substituted mono-amino Zn(II) phthalocyanine, *Dalton Trans.*, 2017, **46**, 1914–1926.
- 13 N. Nishiyama, A. Iriyama, W.-D. Jang, K. Miyata, K. Itaka, Y. Inoue, H. Takahashi, Y. Yanagi, Y. Tamaki, H. Koyama and K. Kataoka, Light-induced gene transfer from packaged DNA enveloped in a dendrimeric photosensitizer, *Nat. Mater.*, 2005, **4**, 934–941.
- 14 N. Nishiyama, Y. Morimoto, W. D. Jang and K. Kataoka, Design and development of dendrimer photosensitizer-incorporated polymeric micelles for enhanced photodynamic therapy, *Adv. Drug Delivery Rev.*, 2009, **61**, 327–338.
- 15 M. Brasch, A. De La Escosura, Y. Ma, C. Uetrecht, A. J. R. Heck, T. Torres and J. J. L. M. Cornelissen, Encapsulation of phthalocyanine supramolecular stacks into virus-like particles, *J. Am. Chem. Soc.*, 2011, **133**, 6878–6881.
- 16 A. Wang, L. Zhou, K. Fang, L. Zhou, Y. Lin, J. Zhou and S. Wei, Synthesis of novel octa-cationic and non-ionic 1,2-ethanediamine substituted Zn(II) phthalocyanines and their *in vitro* anti-cancer activity comparison, *Eur. J. Med. Chem.*, 2012, **58**, 12–21.
- 17 F. Setaro, M. Brasch, U. Hahn, M. S. T. Koay, J. J. L. M. Cornelissen, A. de la Escosura and T. Torres, Generation-dependent templated self-assembly of biohybrid protein nanoparticles around photosensitizer dendrimers, *Nano Lett.*, 2015, **15**, 1245–1251.
- 18 J. Mikkilä, E. Anaya-Plaza, V. Liljestrom, J. R. Caston, T. Torres, A. de la Escosura and M. A. Kostiaainen, Hierarchical organization of organic dyes and protein cages into photoactive crystals, *ACS Nano*, 2016, **10**, 1565–1571.
- 19 F. Dumoulin, M. Durmuş, V. Ahsen and T. Nyokong, Synthetic pathways to water-soluble phthalocyanines and close analogs, *Coord. Chem. Rev.*, 2010, **254**, 2792–2847.
- 20 E. Anaya-Plaza, A. Aljarilla, G. Beaune, Nonappa, J. V. I. Timonen, A. de la Escosura, T. Torres and M. Kostiaainen, Phthalocyanine-virus nanofibers as heterogeneous catalysts for continuous-flow photo-oxidation processes, *Adv. Mater.*, 2019, 1902582.

- 21 E. Anaya-Plaza, E. van de Winckle, J. Mikkila, J.-M. Malho, O. Ikkala, O. Gulias, R. Bresoli-Obach, M. Agut, S. Nonell, T. Torres, M. A. Kostianen and A. de la Escosura, Photo-antimicrobial biohybrids by supramolecular immobilization of cationic phthalocyanines onto cellulose nanocrystals, *Chem. – Eur. J.*, 2017, **23**, 4320–4326.
- 22 J. A. Gonzalez-Delgado, P. J. Kennedy, M. Ferreira, J. P. C. Tome and B. Sarmiento, Use of photosensitizers in semisolid formulations for microbial photodynamic inactivation, *J. Med. Chem.*, 2016, **59**, 4428–4442.
- 23 H. Cho, J. Gao and G. S. Kwon, PEG-*b*-PLA micelles and PLGA-*b*-PEG-*b*-PLGA sol-gels for drug delivery, *J. Controlled Release*, 2016, **240**, 191–201.
- 24 T. K. Dash and V. B. Konkimalla, Poly- ϵ -caprolactone based formulations for drug delivery and tissue engineering: a review, *J. Controlled Release*, 2012, **158**, 15–33.
- 25 J. W. Hofman, M. G. Carstens, F. van Zeeland, C. Helwig, F. M. Flesch, W. E. Hennink and C. F. van Nostrum, Photocytotoxicity of mTHPC (temoporfin) loaded polymeric micelles mediated by lipase catalyzed degradation, *Pharm. Res.*, 2008, **25**, 2065–2073.
- 26 J. W. H. Wennink, Y. Liu, P. Makinen, F. Setaro, A. de la Escosura, M. Bourajjaj, J. Lappalainen, L. Holappa, J. B. van den Dikkenberg, M. al Fartousi, P. Trohopoulos, S. Yla-Herttua, T. Torres, W. E. Hennink and C. F. van Nostrum, Macrophage selective photodynamic therapy by *meta*-tetra(hydroxyphenyl)-chlorin loaded polymeric micelles: a possible treatment for cardiovascular diseases, *Eur. J. Pharm. Sci.*, 2017, **107**, 112–125.
- 27 Y. Shi, A. Elkhabaz, F. A. Yousef Yengej, J. van den Dikkenberg, W. E. Hennink and C. F. van Nostrum, π - π Stacking induced enhanced molecular solubilization, singlet oxygen production, and retention of a photosensitizer loaded in polymeric micelles, *Adv. Healthcare Mater.*, 2014, **3**, 2023–2031.
- 28 Y.-S. Li, S. I. A. Zaidi, M. A. J. Rodgers, H. Mukhtar, M. E. Kenney, N. L. Oleinick, J. He, H. E. Larkin and B. D. Richter, The synthesis, photophysical and photobiological properties and *in vitro* structure-activity relationships of a set of silicon phthalocyanine PDT photosensitizers, *Photochem. Photobiol.*, 1997, **65**, 581–586.
- 29 H. M. Anula, J. C. Berlin, H. Wu, Y.-S. Li, X. Peng, M. E. Kenney and M. A. J. Rodgers, Synthesis and photophysical properties of silicon phthalocyanines with axial siloxy ligands bearing alkylamine termini, *J. Phys. Chem. A*, 2006, **110**, 5215–5223.
- 30 J. W. Hofman, F. van Zeeland, S. Turker, H. Talsma, S. A. G. Lambrechts, D. V. Sakharov, W. E. Hennink and C. F. van Nostrum, Peripheral and axial substitution of phthalocyanines with solketal groups: synthesis and *in vitro* evaluation for photodynamic therapy, *J. Med. Chem.*, 2007, **50**, 1485–1494.
- 31 X.-J. Jiang, P.-C. Lo, Y.-M. Tsang, S.-L. Yeung, W.-P. Fong and D. K. P. Ng, Phthalocyanine–polyamine conjugates as pH-controlled photosensitizers for photodynamic therapy, *Chem. – Eur. J.*, 2010, **16**, 4777–4783.
- 32 X.-J. Jiang, P.-C. Lo, S.-L. Yeung, W.-P. Fong, D. K. P. Ng and A. pH-responsive, fluorescence probe and photosensitizer based on a tetraamino silicon(IV) phthalocyanine, *Chem. Commun.*, 2010, **46**, 3188–3190.
- 33 J. Li, Y. Yang, P. Zhang, J. R. Sounik and M. E. Kenney, Synthesis, properties and drug potential of the photosensitive alkyl- and alkylsiloxy-ligated silicon phthalocyanine Pc 227, *Photochem. Photobiol. Sci.*, 2014, **13**, 1690–1698.
- 34 C. Farren, C. A. Christensen, S. FitzGerald, M. R. Bryce and A. Beeby, Synthesis of novel phthalocyanine–tetrathiafulvalene hybrids; Intramolecular fluorescence quenching related to molecular geometry, *J. Org. Chem.*, 2002, **67**, 9130–9139.
- 35 K. K.-H. Wang, J. D. Wilson, M. E. Kenney, S. Mitra and T. H. Foster, Irradiation-induced enhancement of Pc 4 fluorescence and changes in light scattering are potential dosimeters for Pc 4 PDT, *Photochem. Photobiol.*, 2007, **83**, 1056–1062.
- 36 F. J. Céspedes-Guirao, L. M. Gomis, K. Ohkubo, S. Fukuzumi, F. Fernández-Lázaro and A. S. Santos, Synthesis and photophysics of silicon phthalocyanine–perylenebisimide hybrids connected through rigid and flexible bridges, *Chem. – Eur. J.*, 2011, **17**, 9153–9163.
- 37 T. Doane, A. Chomas, S. Srinivasan and C. Burda, Observation and photophysical characterization of silicon phthalocyanine J-aggregate dimers in aqueous solution, *Chem. – Eur. J.*, 2014, **20**, 8030–8039.
- 38 N. Nombona, K. Maduray, E. Antunes, A. Karsten and T. Nyokong, Synthesis of phthalocyanine conjugates with gold nanoparticles and liposomes for photodynamic therapy, *J. Photochem. Photobiol., B*, 2012, **107**, 35–44.
- 39 N. Kuznetsova, N. S. Gretsova, E. A. Kalmykova, E. A. Makarova, S. N. Dashkevich, V. M. Negrimovskii, O. L. Kaliya and E. A. Lukyanets, Relationship between the photochemical properties and structure of porphyrins and related compounds, *Russ. J. Gen. Chem.*, 2000, **70**, 133–140.
- 40 *Photosensitizers in Medicine, Environment and Security*, ed. T. Nyokong and V. Ahsen, Springer, 2012.
- 41 E. D. Baron, C. L. Malbasa, D. Santo-Domingo, P. Fu, J. D. Miller, K. K. Hanneman, A. H. Hsia, N. L. Oleinick, V. C. Colussi and K. D. Cooper, Silicon phthalocyanine (Pc 4) photodynamic therapy is a safe modality for cutaneous neoplasms: results of a phase 1 clinical trial, *Lasers Surg. Med.*, 2010, **42**, 728–735.
- 42 F. Würthner, T. E. Kaiser and C. R. Saha-Möller, J-aggregates: from serendipitous discovery to supramolecular engineering of functional dye materials, *Angew. Chem., Int. Ed.*, 2011, **50**, 3376–3410.
- 43 P. Libby, Inflammation in atherosclerosis, *Nature*, 2002, **420**, 868–874.
- 44 G. Marelli, A. Sica, L. Vannucci and P. Allavena, Inflammation as target in cancer therapy, *Curr. Opin. Pharmacol.*, 2017, **35**, 57–65.